

Nanoscience & Nanotechnology

Characterization of Ferroelectric Endurance in $\text{Hf}_{0.5}\text{Zr}_{0.5}\text{O}_2$ Deposited by Plasma-enhanced ALD	84
Robust DNA-patterned Glass Surfaces with Micrometer Features by Photolithography and Click Chemistry.	85
Engineering Defects in Remote Epitaxial III-V Materials Grown on Thin Amorphous Carbon	86
Correlated Insulator and Chern Insulators in Rhombohedral Pentalayer Graphene.....	87
The Oxidation Sequence of Ultrathin Hafnium Metal on Graphene	88
Orbital Multiferroicity in Rhombohedral Pentalayer Graphene	89
Tailoring Light Emission and Scattering from Atomically Thin Materials with Transferable Nanostructures	90
Cascaded Compression of Size Distribution of Nanopores in Monolayer Graphene.....	91
Fractional Quantum Anomalous Hall Effect in Graphene	92
Towards Uniform Probabilistic Distribution in Superparamagnetic Tunnel Junctions	93
Tunable Mechanical Response of Self-Assembled Nanoparticle Superlattices	94
Novel Tellurium Contacts for P-type WSe_2 Devices.....	95
Optimizing the Radiative Lifetimes of Perovskite Nanocrystals for Quantum Emission Applications.....	96
3D-Printed, Non-Planar Electron Sources for Projection Lithography	97
Designer Ultrathin Resonators using Delamination Lithography	98
Rewiring Photosynthesis.....	99
Parameters Extraction for a Superconducting Thermal Switch (hTron) SPICE Model	100
Unconventional Ferroelectricity in Moiré Heterostructure.....	101
Elucidating the Dominant Exciton Dynamics in MOCs through Physical, Chemical, and Electrical Manipulation of the Lattice.....	102
Universal Transferred Process for 2D Materials	103
Defects Break the Self-Limiting Nature of the Room-Temperature Atomic-Layer Substitution for Growing Janus Monolayer Transition Metal Dichalcogenides	104
Elucidating the Role of MOF Pore Size on OSN Performance of Microporous Polymer-based Mixed-matrix Membranes	105
Implementation of Multi-functional Diffractive Optical Elements by Implosion Fabrication	106
Large Quantum Anomalous Hall Effect in Spin-orbit Proximitized Rhombohedral Graphene.....	107

Characterization of Ferroelectric Endurance in $\text{Hf}_{0.5}\text{Zr}_{0.5}\text{O}_2$ Deposited by Plasma-enhanced ALD

T. E. Espedal, Y. Shao, E. R. Borujeny, J. A. del Alamo

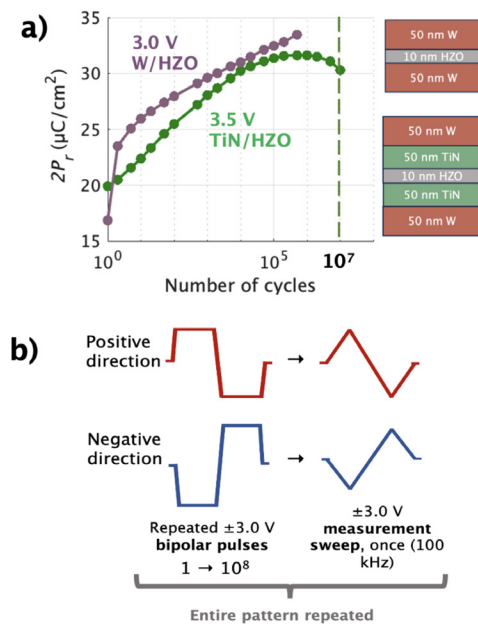
Sponsorship: MIT Undergraduate Research Opportunity Program, Intel Corporation, Semiconductor Research Corporation

Among different non-volatile memory (NVM) technologies, ferroelectric (FE) memory based on complementary metal-oxide semiconductor- (CMOS) compatible $\text{Hf}_{0.5}\text{Zr}_{0.5}\text{O}_2$ (HZO) has emerged as one of the most promising, as it could potentially provide low-voltage operation, fast switching, long data retention, and high device endurance. Plasma-enhanced atomic layer deposition (PEALD) has shown film quality that might lead to improved memory behavior in HZO. However, a detailed study of endurance in PEALD HZO, and more importantly the role of various process conditions, is needed. In this work, we study the endurance characteristics of PEALD HZO in a capacitor configuration, processed with different metal electrode W or TiN, Figure 1.

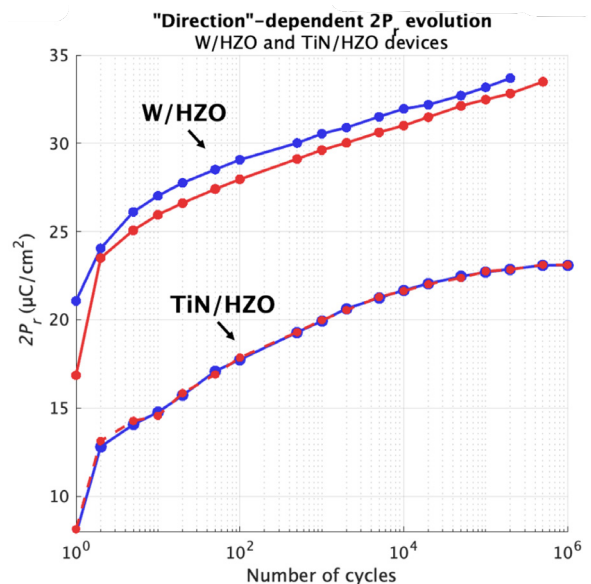
We study the endurance characteristics by applying 3.0 V bipolar pulses followed by a triangular diagnostic waveform, from which we extract remnant polarization (Figure 2) and coercive field. Using a pulse

amplitude of 3.0V, TiN devices yield a lower remnant polarization than W devices, since the 3.0 V voltage applied is a suitable value for W devices but relatively low for TiN. We also observe symmetric wakeup in TiN devices, compared to asymmetric wakeup in W devices under the same conditions (Figure 2). This indicates different changes in the respective metal/HZO interfaces that appear with repeated cycling. Furthermore, we observe early breakdown in W devices without apparent fatigue (Figure 2), while we see clear wake-up and fatigue stages with much longer endurance cycles ($>10^7$ for 3.5 V; Figure 1) in TiN counterparts.

Our work shows that the choice of metal in a FE HZO structure has significant effects on device wake up and endurance. Analyzing these effects is important for identifying the optimal HZO device structure and process conditions for eventual NVM applications.



▲ Figure 1: a) Endurance of W/HZO and TiN/HZO at 3.0V and 3.5V, respectively; the last point measured is just before device breakdown. Note the presence of fatigue in TiN/HZO devices. On the right, schematic of device structure. b) Measurement scheme for cycled endurance V-t.



▲ Figure 2: Evolution of remnant polarization, $2P_r$, dependent on direction of ± 3.0 V bipolar pulse cycling and ± 3.0 V triangular I-V measurement sweep.

Robust DNA-patterned Glass Surfaces with Micrometer Features by Photolithography and Click Chemistry.

E. Perry, J. Tiepelt, J. Jacobson
Sponsorship: Media Lab Consortia

The ability to precisely pattern DNA onto glass is paramount for various bio-analytical applications, including DNA microarrays, biosensors, microfluidics, next-generation sequencing, and lab-on-a-chip. Contemporary fabrication techniques often employ printing technologies such as inkjet, piezoelectric, and contact printing for precise droplet placement followed by chemical immobilization. Alternatively, photolithographic exposure can activate or deactivate custom-designed regions of the surface to be patterned with biomolecules. DNA immobilization unto the glass is commonly achieved by Streptavidin-Biotin interactions or the use of silanized surfaces. Both methods are well established yet carry certain disadvantages and complexities, specifically when combined with advanced microfabrication processes to generate micron and submicron patterns.

In this work, we propose a novel method to fabricate robust DNA-patterned glass surfaces with

micron-scale features. The innovation in this approach is the combination of copper-free click chemistry with a biocompatible photolithographic process. Copper-free click chemistry is based on the reaction of diaryl cyclooctene (DBCO) with an azide-labeled reaction partner. In our process, azide-coated glass is first masked by direct-write photolithography followed by plasma ashing, to generate reactive azide regions underneath the photomask. Room-temperature suspension of DNA molecules modified with DBCO leads to covalent attachment of DNA strictly to the active regions. Our preliminary results show this process generates patterned surfaces with a very high signal-to-noise ratio compared to standard techniques, as well as stability and resistance to denaturing conditions. Our method could appeal to researchers interested in custom in-house fabrication of pristine DNA-coated surfaces.

FURTHER READING:

- *H. Lee, J. Cañada, and L. F. Velásquez-García, "Compact Peristaltic Vacuum Pumps via Multi-material Extrusion," *Additive Manufacturing*, vol. 68, p. 103511, 2023, ISSN 2214-8604, <https://doi.org/10.1016/j.addma.2023.103511>.
- H. Lee and L. F. Velásquez-García, "3D-Printed, Peristaltic Vacuum Pumps for Compact Applications," *2022 21st International Conference on Micro and Nanotechnology for Power Generation and Energy Conversion Applications (PowerMEMS)*, pp. 162-165, 2022, doi: 10.1109/PowerMEMS56853.2022.10007548.
- D. Melo Máximo and L. F. Velásquez-García, "Additively Manufactured Electrohydrodynamic Ionic Liquid Pure-ion Sources for Nanosatellite Propulsion," *Additive Manufacturing*, vol. 36, p. 101719, 2020, doi: 10.1016/j.addma.2020.101719.

Engineering Defects in Remote Epitaxial III-V Materials Grown on Thin Amorphous Carbon

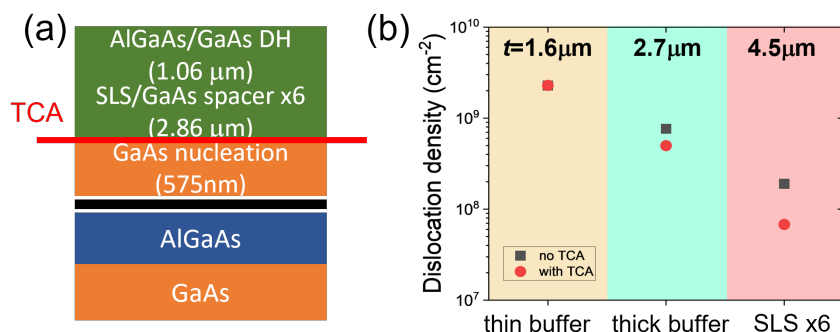
N. M. Han, K. Lu, H. Kim, S. Cho, J. Kim

Sponsorship: Defense Advanced Research Projects Agency, United States Air Force Research Laboratory, Department of Energy, Rohm Semiconductor, LG, Umicore, Universiti Tenaga Nasional

Remote epitaxy has emerged as a facile technique for producing freestanding, wafer-scale membranes of single-crystalline semiconductors. However, it still encounters challenges but also presents other benefits when compared to direct epitaxy. In the case of growing epitaxial layers on the same or lattice-matched substrates, remote epitaxy results in lower material quality and higher defect density due to the attenuated atomic registry from the substrate. To address this issue, we propose the incorporation of thermal cycle annealing (TCA) and strained layer superlattice (SLS) into the growth process, as illustrated in Figure 1a, which effectively reduces the threading dislocation density by a few orders of magnitude, as shown in Figure 1b.

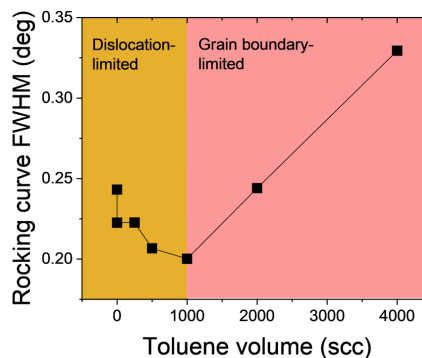
Conversely, when the substrate and epitaxial layer have a high lattice mismatch, remote epitaxy offers an advantage through the van der Waals interface, which provides an additional pathway to relax the strain

developed in heteroepitaxial layers. This spontaneous relaxation mechanism significantly reduces the occurrence of misfit dislocations that are commonly observed in direct heteroepitaxy. By directly growing thin amorphous carbon (TAC) on GaAs, by-passing the need for a 2D layer transfer process, we can create an ultra-thin van der Waals interface that enhances the atomic registry of the epitaxial layer to the substrate while facilitating strain relaxation. In this study, we investigate the impact of TAC growth time on the material quality of remote heteroepitaxial InGaAs layers grown on GaAs substrates, as shown in Figure 2. The inherent strain relaxation capabilities offered by remote epitaxy enable the heteroepitaxy of high-quality membranes on lattice-mismatched substrates, paving the way for the fabrication of diverse electronic and optoelectronic devices.



◀ Figure 1: (a) Schematic of thermal cycle annealing (TCA) and strained-layer superlattice (SLS) and (b) their influence on the dislocation density of remote-epitaxial GaAs.

▶ Figure 2: Effect of in-situ grown graphene thickness, represented by volume of toluene precursor flown, on quality of InGaAs grown on GaAs substrate (low rocking curve full width at half maximum indicates better quality).



FURTHER READING

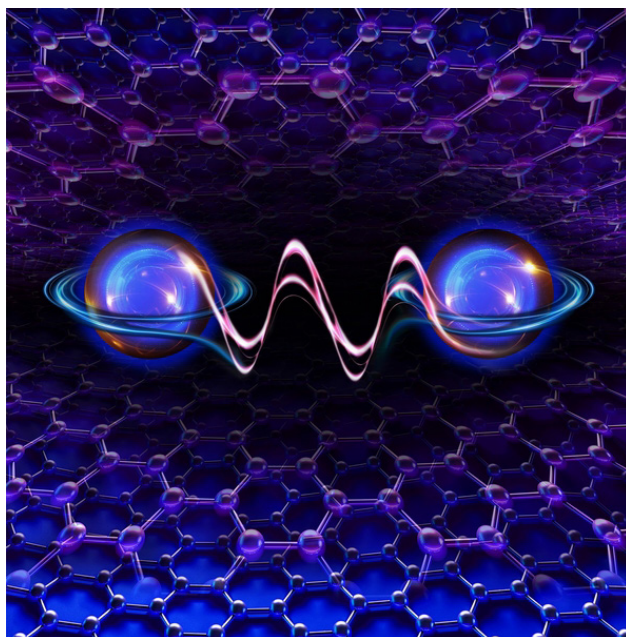
- D. Jung et al. "Low Threading Dislocation Density GaAs Growth on On-axis GaP/Si (001)," *J. Appl. Phys.*, vol. 122, p. 225703, 2017.
- S. H. Bae et al. "Graphene-assisted Spontaneous Relaxation Towards Dislocation-free Heteroepitaxy," *Nature Nanotechnology*, vol. 15, p. 272, 2020.

Correlated Insulator and Chern Insulators in Rhombohedral Pentalayer Graphene

T. Han, Z. Lu, G. Scuri, J. Sung, J. Wang, T. Han, K. Watanabe, T. Taniguchi, L. Fu, H. Park, L. Ju
Sponsorship: Sloan Fellowship, NSF

Rhombohedral-stacked multilayer graphene hosts a pair of flat bands touching at zero energy, which should give rise to correlated electron phenomena that can be tuned further by an electric field. Moreover, when electron correlation breaks the isospin symmetry, the valley-dependent Berry phase at zero energy may give rise to topologically non-trivial states. Here we measure electron transport through hexagonal boron nitride-encapsulated pentalayer graphene down to 100 mK. We observed a correlated insulating state with resistance at the megaohm level or greater at charge density $n=0$ and displacement field $D=0$. Tight-binding calculations predict a metallic ground state under

these conditions. By increasing D , we observed a Chern insulator state with $C=-5$ and two other states with $C=-3$ at a magnetic field of around 1 T. At high D and n , we observed isospin-polarized quarter- and half-metals. Hence, rhombohedral pentalayer graphene exhibits two different types of Fermi-surface instability, one driven by a pair of flat bands touching at zero energy, and one induced by the Stoner mechanism in a single flat band. Our results establish rhombohedral multilayer graphene as a suitable system for exploring intertwined electron correlation and topology phenomena in natural graphitic materials without the need for moiré superlattice engineering.



▲ Figure 1. Resistance of rhombohedral pentalayer graphene as function of charge density and gate-displacement field. Blue dot corresponds to correlated insulator state; purple and yellow dots correspond to quarter and half-metals, respectively. Red star corresponds to valley-polarized metal state.

FURTHER READING

- T. Han, Z. Lu, G. Scuri, J. Sung, J. Wang, T. Han, K. Watanabe, T. Taniguchi, et al. "Correlated Insulator and Chern Insulators in Pentalayer Rhombohedral-stacked Graphene," *Nat. Nanotechnol.* vol. 19, pp. 181–187, 2024. <https://doi.org/10.1038/s41565-023-01520-1>

The Oxidation Sequence of Ultrathin Hafnium Metal on Graphene

Z. Liu, R. Jaramillo, F. M. Ross
Sponsorship: SRC (Contract No. 2021-NM-3027)

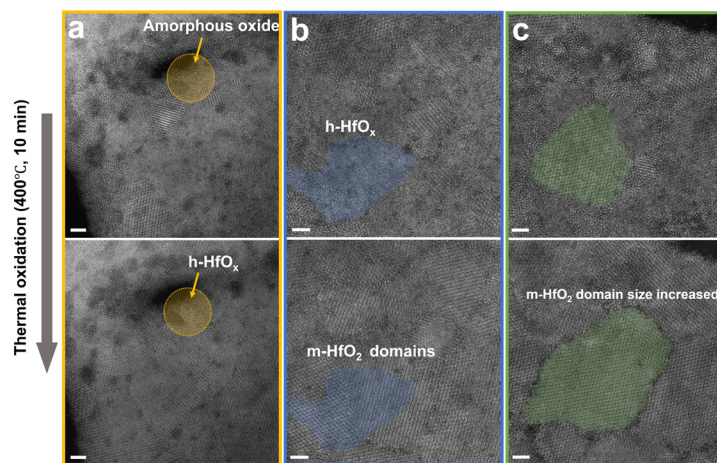
Hafnium oxides with their rich crystal phases are an important family of electronic materials based on their high dielectric constants, ferroelectric properties, and application in resistive switching random access memory. Understanding the oxidation of ultrathin hafnium (Hf) film at the atomic level will offer opportunities for the phase engineering of hafnium oxides towards different applications.

Here, starting with the epitaxial deposition of Hf on graphene carried out in ultra-high vacuum, we demonstrate that exposure to air at room temperature for only a few minutes results in the formation of several oxide phases (Figure 1, top row). These are an amorphous oxide, a hexagonal structure (h-HfO_x), and a monoclinic HfO₂ (m-HfO₂). We find the h-HfO_x phase to be intermediate in composition and structure between hcp Hf and m-HfO₂. The m-HfO₂ exhibits three equivalent orientations on the Hf crystal, which can be understood through its lower structural symmetry compared to the parent Hf hexagonal close packed (hcp) structure.

Further thermal oxidation of samples displaying these three structures results in the crystallization of some amorphous regions into h-HfO_x and conversion

of the amorphous and hexagonal structures to m-HfO₂ (Figure 1, bottom row). Based on the crystallographic orientation relations observed, for the conversion of Hf to m-HfO₂ it is necessary for the stacking sequence of Hf layers in the out-of-plane direction to change from the AB stacking of hcp Hf to the ABC stacking of m-HfO₂. We expect this change in stacking sequence to lead to the appearance of a hexagonal pattern when imaged. We therefore propose that h-HfO_x, which displays a hexagonal pattern, contains sequences of AB and ABC stacked Hf layers in the out-of-plane direction.

By examining the structural changes and hence the atomic oxidation mechanism of ultrathin Hf using electron microscopy, we aim to clarify the opportunities for achieving phase control of hafnium oxides. These results are also relevant to solving the key issue of scalable formation of a conformal dielectric on two-dimensional (2D) materials such as graphene or transition metal dichalcogenides, by separating the growth process into first obtaining epitaxy between the metal and 2D material, followed by epitaxy of the oxide layer.



▲ Figure 1: Oxide transitions during thermal oxidation, observed before and after thermal oxidation by scanning transmission electron microscopy (STEM). (a) Crystallization of amorphous oxides into h-HfO_x. (b) Conversion from h-HfO_x to m-HfO₂. (c) STEM images showing the transformation of larger m-HfO₂ grains.

FURTHER READING

- Z. Liu, R. Jaramillo, and F. M. Ross, "The Oxidation Sequence of Ultrathin Hafnium Metal on Graphene," *Microscopy and Microanalysis*, 2024, in press.
- K. Reidy, J. D. Thomsen, H. Y. Lee, V. Zarubin, Y. Yu, B. Wang, T. Pham, P. Periwal, et al., "Mechanisms of Quasi van der Waals Epitaxy of Three-Dimensional Metallic Nanoislands on Suspended Two-Dimensional Materials," *Nano Letters*, vol. 22, pp. 5849-5858, Jul. 2022.

Orbital Multiferroicity in Rhombohedral Pentlayer Graphene

T. Han, Z. Lu, G. Scuri, J. Sung, J. Wang, T. Han, K. Watanabe, T. Taniguchi, L. Fu, H. Park, L. Ju
Sponsorship: Sloan Fellowship, NSF

Ferroic orders describe spontaneous polarization of spin, charge, and lattice degrees of freedom in materials. Materials exhibiting multiple ferroic orders, known as multiferroics, play important roles in multifunctional electrical and magnetic device applications. Two-dimensional materials with honeycomb lattices offer opportunities to engineer unconventional multiferroicity, in which the ferroic orders are driven purely by the orbital degrees of freedom and not by electron spin. These include ferro-valleytricity corresponding to the electron valley and ferro-orbital-magnetism supported by quantum geometric effects. These orbital multiferroics could offer strong valley-magnetic couplings and large responses to external fields, enabling device applications such as multiple-state memory elements and electric control of the valley and magnetic states.

We observed orbital multiferroicity in pentlayer

rhombohedral graphene using low-temperature magneto-transport measurements. We observed anomalous Hall signals R_{xy} with an exceptionally large Hall angle ($\tan\theta_H > 0.6$) and orbital magnetic hysteresis at hole doping. Four such states exist with different valley polarizations and orbital magnetizations, forming a valley-magnetic quartet. By sweeping the gate electric field E , we observed a butterfly-shaped hysteresis of R_{xy} connecting the quartet. This hysteresis indicates a ferro-valleytronic order that couples to the composite field $E \cdot B$ (where B is the magnetic field), but not to individual fields. Tuning E would switch each ferroic order independently and achieve non-volatile switching of them together. Our observations demonstrate a previously unknown type of multiferroics and point to electrically tunable ultralow-power valleytronic and magnetic devices.

FURTHER READING

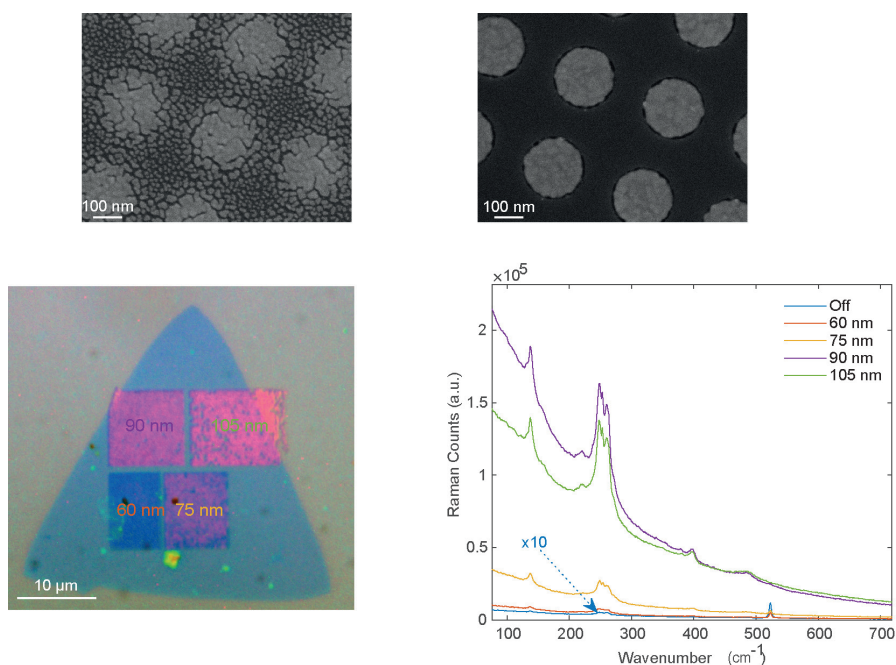
- T. Han, Z. Lu, G. Scuri, et al. "Orbital Multiferroicity in Pentlayer Rhombohedral Graphene," *Nature*, vol. 623, pp. 41–47, 2023. "<https://doi.org/10.1038/s41586-023-06572-w>"<https://doi.org/10.1038/s41586-023-06572-w>

Tailoring Light Emission and Scattering from Atomically Thin Materials with Transferable Nanostructures

A. K. Demir, J. Li, T. Zhang, C. Occhialini, L. Nessi, J. Kong, R. Comin

Sponsorship: U.S. Department of Energy, Office of Science National Quantum Information Science Research Center's Co-design Center for Quantum Advantage (C2QA) under contract number DE-SC0012704, Raith VELION FIB-SEM in the MIT nano Characterization Facilities (Award: DMR-2117609), MathWorks Science Fellowship (Award: 4000182189)

Optical spectroscopy is indispensable for unveiling the unique properties and symmetries of materials in the atomically thin limit. However, the vanishing thickness often leads to a cross section too low for conventional optical methods to work. In this work, we developed a technique, completely dry and simple to implement, to fabricate and transfer high-resolution optical enhancement nanostructures for Raman and PL spectroscopy. We demonstrate orders-of-magnitude increase in the intensities of single-layer WSe_2 phonon modes; enabling the detection of phonon modes of three-layer NiI_2 using non-resonant excitation; and selective Purcell enhancement of the quenched excitons in $\text{WSe}_2/\text{MoS}_2$ heterostructures. We also highlight that the method is particularly suitable for optical studies of air-sensitive materials, as the fabrication and transfer can be performed in situ.



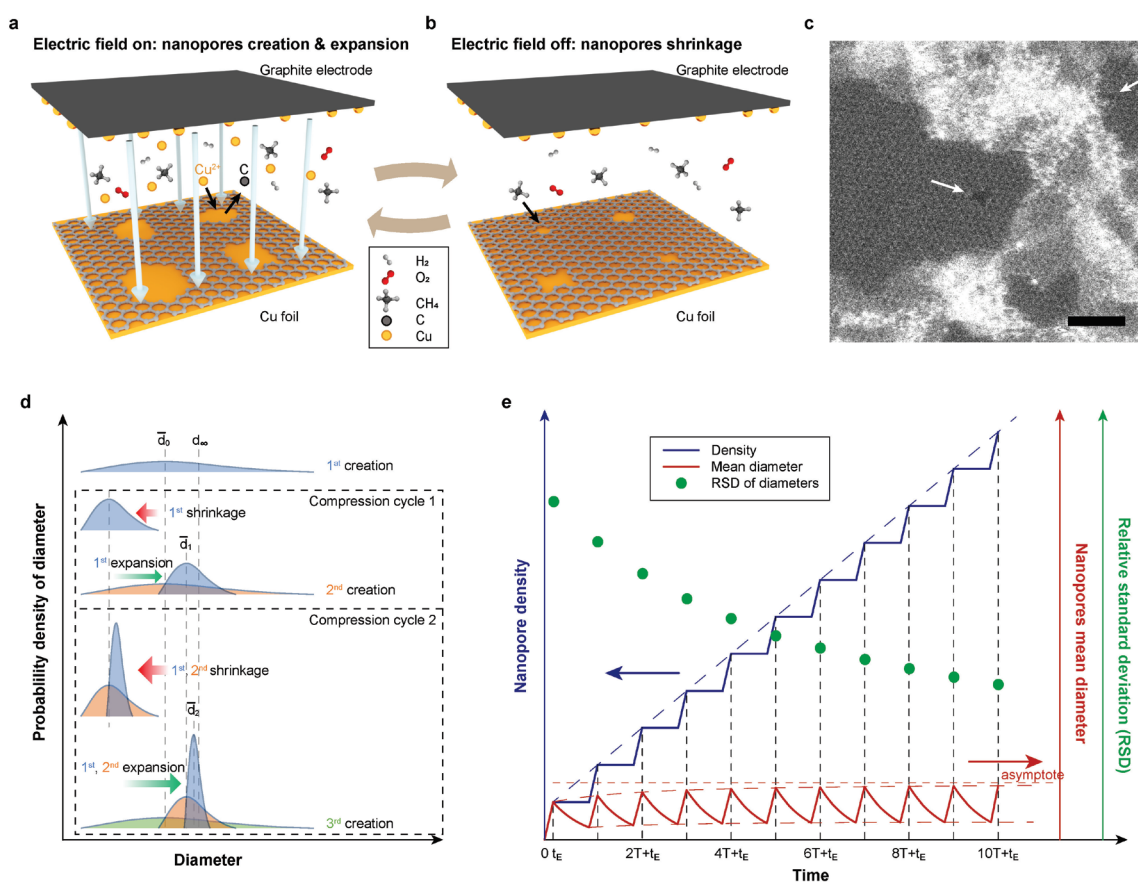
▲ Figure 1: Top Panel: Our method provides significant increase in the quality of the nanostructures fabricated without adhesion layers. Bottom Panel: Lack of the adhesion layer enables us to transfer the nanostructures on van der Waals materials, resulting in a large enhancement of the optical signal.

Cascaded Compression of Size Distribution of Nanopores in Monolayer Graphene

J. Wang, C. Cheng, X. Zheng, T. Zhang, J. Kong
Sponsorship: U.S. Army Research Office, U.S. Department of Energy

Monolayer graphene, featuring nanometre-scale pores and exceptional mechanical properties, is ideal for ion/molecular separations, energy storage, and electronics. Precise engineering of nanopore size and distribution is crucial for these applications. Top-down methods typically result in log-normal size distributions with long tails, especially at subnanometre scales, and a trade-off between nanopore size distribution and density limits their practical use. Here, we report a cascaded compression method for producing graphene nanopores with a narrowed, left-skewed size distribution and ul-

trashort tail deviation (Fig. 1). This process involves sequential steps where existing nanopores undergo both shrinkage and expansion, simultaneously creating new nanopores and enhancing overall density. The result is graphene nanopores with high density, left-skewed distribution, enabling ultrafast, size-tunable transport of ions and molecules. This technique offers independent control over nanopore density, diameter, deviation, and distribution skewness, potentially revolutionizing nanotechnology.



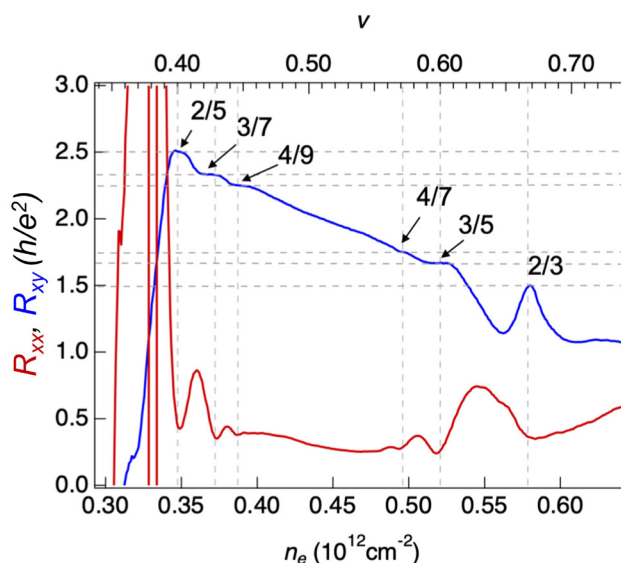
▲ Figure 1: Cascaded compression cycles. a, Creation & expansion of nanopores by Cu sputter. b, Shrinkage of nanopores by regrowth. c, STEM image of nanopores. Scale bar, 2 nm. The schematic evolution of d, the probability density of diameter, and e, nanopore density, mean diameter, and RSD vs. time.

Fractional Quantum Anomalous Hall Effect in Graphene

Z. Lu, T. Han, Y. Yao, A. P. Reddy, J. Yang, J. Seo, K. Watanabe, T. Taniguchi, L. Fu, L. Ju
Sponsorship: Sloan Fellowship, NSF

The fractional quantum anomalous Hall effect (FQAHE), the analogue of the fractional quantum Hall effect at zero magnetic field, is predicted to exist in topological flat bands under spontaneous time-reversal-symmetry breaking. The demonstration of the FQAHE could lead to non-Abelian anyons that form the basis of topological quantum computation. So far, the FQAHE has been observed only in twisted MoTe_2 at a moiré filling factor $\nu > 1/2$. Graphene-based moiré superlattices are believed to host the FQAHE with the potential advantage of superior material quality and higher electron mobility. Here we report the observation of integer and fractional QAH effects in a rhombohedral pentalayer graphene-hBN moiré superlattice. At zero

magnetic field, we observed plateaus of quantized Hall resistance $R_{xy} = h/(e^2\nu)$ at $\nu = 1, 2/3, 3/5, 4/7, 4/9, 3/7$, and $2/5$ of the moiré superlattice, respectively, accompanied by clear dips in the longitudinal resistance R_{xx} . R_{xy} equals $2h/e^2$ at $\nu = 1/2$ and varies linearly with ν , similar to the composite Fermi liquid in the half-filled lowest Landau level at high magnetic fields. By tuning the gate-displacement field D and ν , we observed phase transitions from composite Fermi liquid and FQAH states to other correlated electron states. Our system provides an ideal platform for exploring charge fractionalization and (non-Abelian) anyonic braiding at zero magnetic field, especially considering a lateral junction between FQAHE and superconducting regions in the same device.



▲ Figure 1: R_{xx} and R_{xy} in the rhombohedral pentalayer graphene/hBN moiré superlattice. Clear plateaus of R_{xy} at $5h/(2e^2)$, $7h/(3e^2)$, $9h/(4e^2)$, $7h/(4e^2)$, $5h/(3e^2)$ and $3h/(2e^2)$ emerge at filling factor $\nu = 2/5, 3/7, 4/9, 4/7, 3/5$ and $2/3$, as indicated by the dashed lines and arrows. R_{xx} shows clear dips at the corresponding filling factors. These fractional states host fractionally charged quasiparticles with fractional statistics.

FURTHER READING

- Z. Lu, T. Han, Y. Yao, et al. "Fractional Quantum Anomalous Hall Effect in Multilayer Graphene," *Nature*, vol. 626, pp. 759–764, 2024. <https://doi.org/10.1038/s41586-023-07010-7>

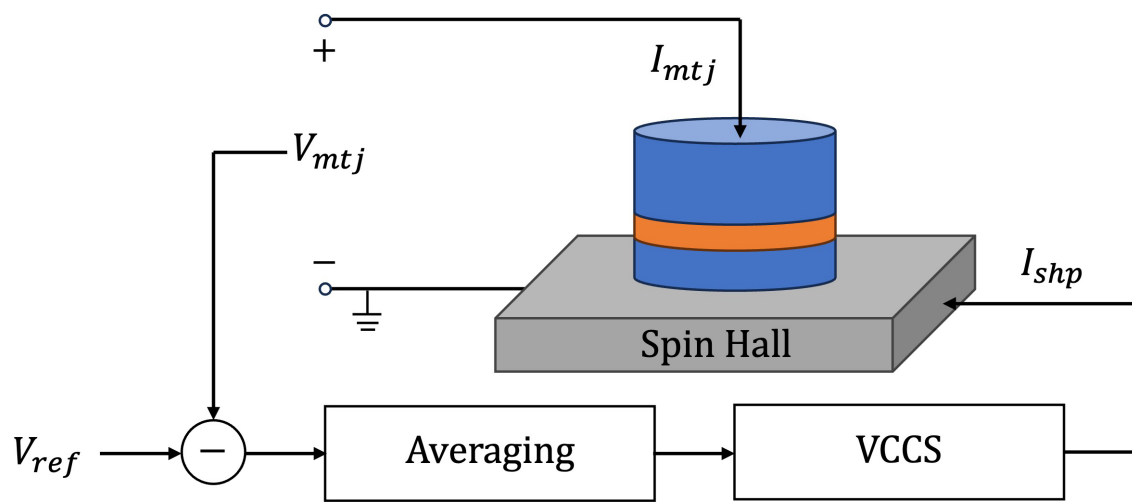
Towards Uniform Probabilistic Distribution in Superparamagnetic Tunnel Junctions

D. Koh, B. C. McGoldrick, L. Liu, M. A. Baldo

Sponsorship: Semiconductor Research Corporation Supreme #3137.009

Stochastic algorithms, which employ statistical methods with random numbers, are prevalent in fields such as cryptography and machine learning. Conventional computers, however, produce random bitstreams via pseudo-random number generators. These bitstreams, while appearing random, actually possess long-range orders, reducing their effectiveness for many stochastic algorithms. Superparamagnetic tunnel junctions have emerged as candidates for scalable and energy-efficient true random number generators. Yet, achieving

a uniform probabilistic distribution, a critical requirement for most stochastic algorithms, is challenging with a single nanomagnet. In this work, we explore an approach to enforce a uniform distribution in the device's probabilistic output and assess its impact on the true randomness. This method not only promises faster and more energy-efficient random number generation but also opens possibilities for integrating massive stochastic nanomagnets into large-scale systems.



▲ Figure 1: Conceptual diagram of controlling probability distribution by utilizing current-induced spin-orbit-torques in three-terminal superparamagnetic tunnel junctions.

Tunable Mechanical Response of Self-Assembled Nanoparticle Superlattices

S. Dhulipala, D. Yee, Z. Zhou, R. Sun, J. E. Andrade, R. J. Macfarlane, C. M. Portela

Sponsorship: National Science Foundation (NSF) CAREER Award CMMI-2142460, U.S. Army Research Office under Grant W911NF-18-1-0197, NSF CAREER Award CHE-1653289, and the Department of the Navy, Office of Naval Research, under ONR award number N00014-22-1-2148

Self-assembled nanoparticle superlattices (NPSLs) are an emergent class of self-architected nanocomposite materials that possess promising properties arising from precise nanoparticle ordering. Their multiple coupled properties make them desirable as functional components in devices where mechanical robustness is critical. However, questions remain about NPSL mechanical properties and how shaping them affects their mechanical response. Here, we perform in-situ nanomechanical experiments that evidence up to an 11-fold increase in stiffness (~ 1.49 to 16.9 GPa) and a 5-fold

increase in strength (~ 88 to 426 MPa) because of surface stiffening/strengthening from shaping these nanomaterials via focused-ion-beam (FIB) milling. To predict the mechanical properties of shaped NPSLs, we present discrete element method (DEM) simulations and an analytical core-shell model that captures the FIB-induced stiffening response. This work presents a route for tunable mechanical responses of self-architected NPSLs and provides two frameworks to predict their mechanical response and guide the design of future NPSL-containing devices.

Novel Tellurium Contacts for P-type WSe₂ Devices

H. W. Lee, J. Zhu, K. Reidy, F. Ross, J. Kong, T. Palacios
Sponsorship: Intel (ISRA)

Since the first discovery of graphene, extensive research on two-dimensional (2D) materials has opened promising possibilities for elevating 2D semiconductor applications from the academic to the industrial level for the next generation of electronics. Now, 2D semiconductors can be grown at a large scale, processed using CMOS-compatible fabrication techniques, and demonstrate high-performance transistors with low contact resistance. However, these remarkable improvements have mainly been achieved with n-type 2D semiconductors, primarily focusing on molybdenum disulfide (MoS₂). In the case of p-type 2D semiconductors, such as tungsten diselenide (WSe₂), there are still significant challenges in material growth and reducing contact resistance to make them comparable to n-type 2D transistors. These challenges hinder the demonstration of 2D complementary metal-oxide-semiconductor (CMOS) circuits at an industrial level. In particular, reducing the contact resistance between a p-type 2D

channel and a metal contact is essential to achieving high-performance p-type transistors.

In this work, we explore the use of semimetal tellurium (Te) as contacts for p-type WSe₂ transistors. Semimetals such as bismuth (Bi) and antimony (Sb) are known to mitigate the Fermi level pinning effect at the interface between the metal and MoS₂, thereby drastically reducing the contact resistance of MoS₂ transistors [1]. We compare the performance of WSe₂ transistors with various contact materials, including Te, palladium (Pd), and platinum (Pt), and observe that Te contacts indeed reduce the Fermi level pinning effect at the interface of WSe₂ and Te. In addition, we enhance the performance of WSe₂ transistors by adjusting the deposition temperature of Te. This research on semimetal Te contacts will serve as an important baseline study for novel contacts for p-type 2D transistors, thereby enabling the next generation of commercialized 2D electronic devices.

Optimizing the Radiative Lifetimes of Perovskite Nanocrystals for Quantum Emission Applications

K. McFarlane-Connelly, N. Brown, M. G. Bawendi

Sponsorship: US Department of Energy, Office of Basic Energy Sciences, Division of Materials Sciences and Engineering under award no. DE-SC00216

Realizing practical quantum computing schemes would fundamentally shift our technological capabilities. Imperative to this innovation is the scalable fabrication of quantum emitters (QEs). Ideal QEs approach the transform-limit ratio where the optical coherence lifetime (T_2) of the emission is twice the radiative lifetime (T_1). Large colloidal semiconductor nanocrystals (NCs) are promising QE candidates, however concrete methods of further minimizing their T_1 lifetimes are necessary. While theories have suggested T_1 values might scale inversely proportional to volume, this hypothesis remains unexplored. This research aims to elucidate the impact of size on the quantum emission properties of weakly confined perovskite nanocrystals. By tuning precursor chain lengths, a size series of highly luminescent CsPbBr₃ nanoparticles were prepared with

extremely narrow size distributions. Five distinct sizes of nanocrystals were prepared in the weakly confined regime ranging from 16 to 23 nm, with standard distribution of sizes less than 7%. Post synthetic treatments were employed to boost photoluminescence quantum yields to higher than 80% at room temperature for all samples. The radiative lifetimes of these particles were observed under cryogenic temperatures revealing T_1 values that scaled inversely with particle size, providing experimental confirmation of theoretical predictions. These results demonstrate that increasing particle size is a promising route to approaching the ideal transform limit ratio with NCs. This fundamental work aims to enable future optimization of the quantum emission properties of weakly confined nanocrystals in hopes of realizing a path to scalable quantum emitter materials.

3D-Printed, Non-Planar Electron Sources for Projection Lithography

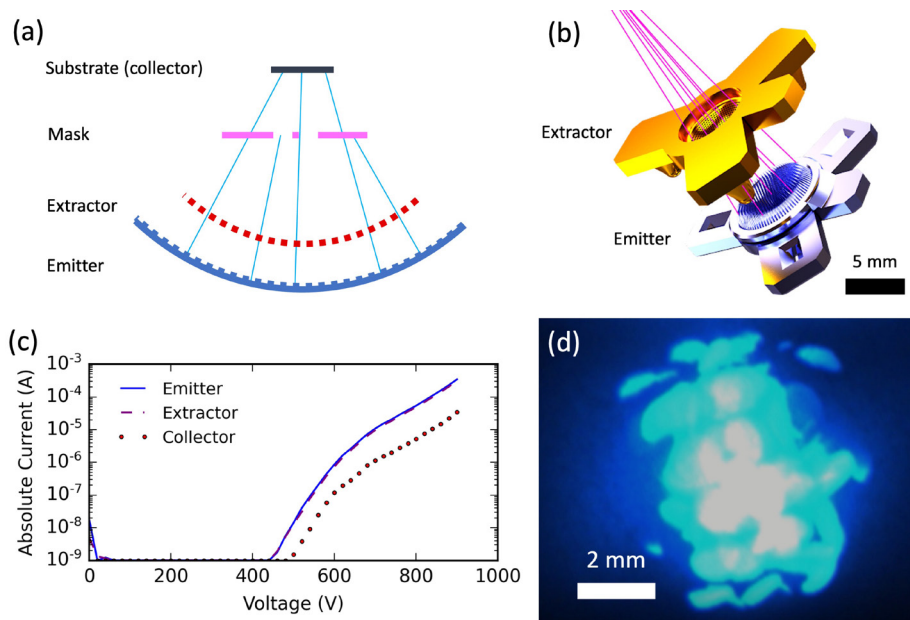
A. Kachkine, C. E. Owens, A. J. Hart, L. F. Velásquez-García

Sponsorship: NewSat Project, COMPETE 2020, ERDF, MIT Portugal Program, Mathworks

Photolithography resolution is diffraction-limited, while electron projection lithography (EPL), though higher resolution, is throughput-limited by electron divergence from planar sources. We report the first non-planar electron sources for EPL, a design paradigm with potential to overcome both limitations.

Fabricated by 3D printing, devices deliver confocal emission, achieving focusing and demagnification. Emission is produced by a concave dish base with an array of carbon nanotube-coated emitters aligned

to the apertures of a concave extractor electrode; both are fabricated by vat photopolymerization 3D printing and modified by subsequent coatings. Our prototype device exhibits a startup voltage of 500 V, a peak emission current of $300 \mu\text{A}/\text{cm}^2$, and a field enhancement factor of $7.8 \times 10^4 \text{ cm}^{-1}$. Phosphor screen imaging of the devices in operation demonstrates that the emission is spatially uniform. Our approach enables compact design at industrial specifications of next-generation EPL systems.



▲ Figure 1: (a) Proposed convex electron source schematic. (b) Device rendering, showing electron paths in pink. (c) Voltage sweep data from device in triode configuration. (d) Phosphor screen image of electron emission.

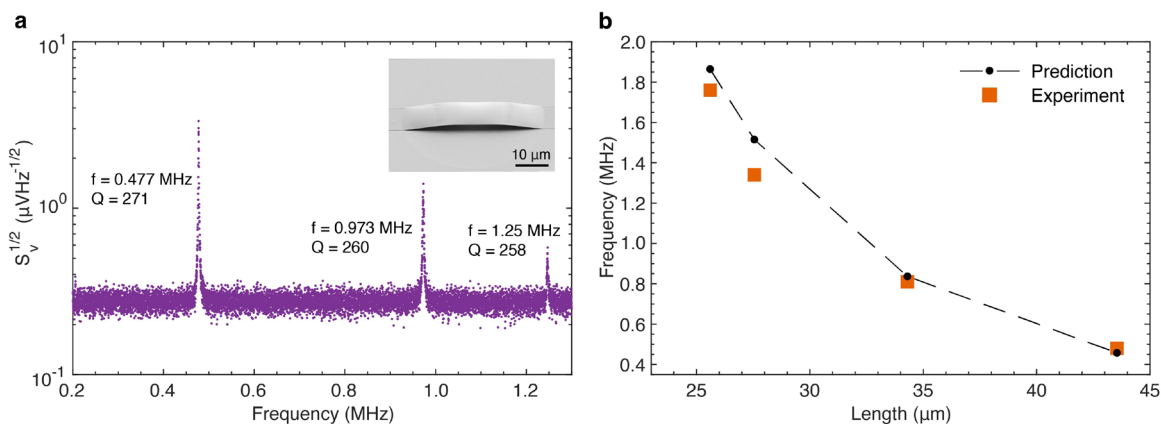
Designer Ultrathin Resonators using Delamination Lithography

S. O. Spector, P. F. Satterthwaite, F. Niroui
Sponsorship: NSF Graduate Research Fellowship

Thin-film, suspended mechanical resonators are a crucial component of nanoelectromechanical systems, from frequency conversion for radio signals to mass spectroscopy for biological sensing. Yet, the inherent instability of conventional, top-down fabrication techniques limits how thin these devices can be made, hampering their sensitivity and potential frequency range.

Here, we show that a nonplanar nanofabrication technique can be used to produce stable, ultrathin mechanical resonators (Figure 1a). By engineering

surface forces using a molecular monolayer and simultaneously controlling the stress in a thin film, three-dimensional “delamination lithography” is achieved. We demonstrate that these devices, which we can design across a broad range of sizes using simple, wafer-scale techniques, conform to their theoretical and simulated behavior (Figure 1b), suggesting applications in designer resonators across frequency orders of magnitude.



▲ Figure 1:(a) First three vibrational modes of a < 30 nm-thin suspended resonator shown in the inset SEM. (b) The fundamental frequency of the resonator as a function of its length, showing a close match between experimentally-measured and simulated results.

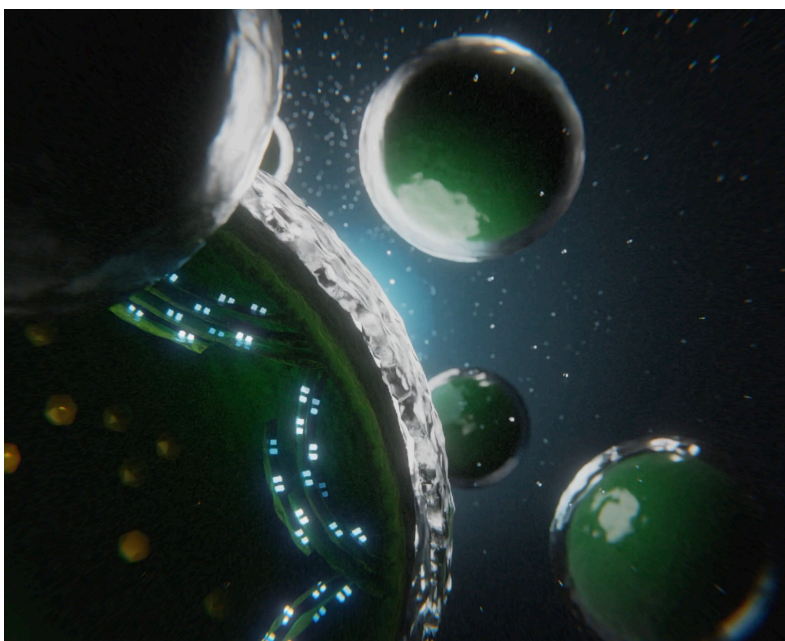
Rewiring Photosynthesis

T. Baikie

Sponsorship: The Lindemann Fellowship

Photosystems II and I (PSII, PSI) are the reaction centre-containing complexes driving the light reactions of photosynthesis. The impressive efficiencies of the photosystems have motivated extensive biological, artificial and biohybrid approaches to 're-wire' photosynthesis for higher biomass-conversion efficiencies and new reaction pathways. Electron extraction at earlier steps, perhaps immediately from photoexcited reaction centres, would enable greater thermodynamic gains; however, this was believed impossible with buried reaction centres. We demonstrate extraction of electrons

directly from photoexcited PSI and PSII. Our results challenge previous models of photoexcited reaction centres and opening new avenues to study and re-wire photosynthesis for biotechnologies and semi-artificial photosynthesis. Here, we demonstrate, using in vivo ultrafast transient absorption (TA) spectroscopy, extraction of electrons directly from photoexcited PSI and PSII at early points (several picoseconds post-photo-excitation) with live cyanobacterial cells or isolated photosystems



▲ Figure 1: Artists impression of cell environment

Parameters Extraction for a Superconducting Thermal Switch (hTron) SPICE Model

V. Karam, O. Medeiros, M. Castellani, R. Foster, T. Dandachi, K. Berggren
Sponsorship: Breakthrough Starshot Initiative, DOE microelectronics

Superconducting nanowire circuits have shown great potential in photon sensing, demonstrating remarkable efficiency in extreme conditions while having large gains and high fanout. Yet, their integration into complex circuits is not as developed as other superconducting technologies. Their scaling is partly limited by a lack of effective simulation tools for superconducting nanowires, preventing designers from getting behavioral insights prior to fabrication.

As circuits increase in size and complexity, the modeling needs to shift from modeling detailed physical interactions to overall behavior of devices. For example, the multilayered heater-nanocryotron (hTron) device – a superconducting nanowire-based switch [1] – which has demonstrated applications in cryogenic memories, neuromorphic computing, and SNSPD array readout [2], was previously simulated

using traditional finite-element modeling (FEM) methods, solving heat diffusion differential equations. However, while FEM techniques simulate individual superconductors accurately, they fall short in simulating larger circuits. Behavioral models are better adapted to that purpose, but require a large number of measurements to accurately reproduce the device's behavior.

In this work, we collect measurement data on the performance of 17 hTron devices and develop a method to extract physical fitting parameters from the measurement curves. Finally, we validate our model by performing the SPICE simulation of a 1:4 hTron-based multiplexer. Our model provides circuit designers with a tool to help understand the hTron's behavior during all design stages, thus promoting broader use of the hTron across various unexplored domains.

FURTHER READING

- R. Baghdadi, et al, "Multilayered Heater Nanocryotron: A Superconducting-nanowire-based Thermal Switch," *Physical Review Applied* 14.5 (2020): 054011.
- B. Oripov, et al, "Thermally Coupled Imager with 400,000 pixels," (2023).

Unconventional Ferroelectricity in Moiré Heterostructure

Z. Zheng, X. Wang, Z. Zhu, S. Carr, T. Devakul, S. C. de la Barrera, N. Paul, Z. Huang, A. Gao, Y. Zhang, D. Bérubé, K. N. Evancho, K. Watanabe, T. Taniguchi, L. Fu, Y. Wang, S.Y. Xu, E. Kaxiras, P. Jarillo-Herrero, Q. Ma
Sponsorship: CATS Program [6950173]

Electronic ferroelectricity represents a new paradigm in which spontaneous symmetry breaking is driven by electronic correlations, in contrast to traditional lattice-driven ferroelectricity, which results in the formation of electric dipoles. Due to its electronic nature, electronic ferroelectricity is expected to exhibit novel characteristics, such as ultrafast switching, large polarization, exceptional durability, and multiple polarization states. However, despite its fundamental interest and technological advantages, switchable electronic ferroelectricity remains exceedingly rare. This abstract will discuss our discovery of a novel electronic ratchet effect in a layer-contrasting graphene-boron nitride moiré heterostructure, which could serve as new evidence of switchable electronic ferroelectricity. Our engineered layer-asymmetric moiré potential

landscapes result in a bipartite electronic system, in which we demonstrate a non-volatile ratcheting behavior tunable by gate voltages. Importantly, the memory states can be stabilized in a quasi-continuous fashion, exhibiting behavior markedly distinct from known ferroelectrics. Our experimental observations, simulations, and theoretical analysis suggest that dipolar excitons could be the driving force and elementary ferroelectric units in our system. This indicates a new type of electronic ferroelectricity where the formation of dipolar excitons with aligned moments generates a macroscopic polarization and leads to an electronically-driven ferroelectric response. Our result could pave the way for innovative quantum analog memory and synaptic devices.

Elucidating the Dominant Exciton Dynamics in MOCs through Physical, Chemical, and Electrical Manipulation of the Lattice

N. J. Samulewicz, W. S. Lee, W. A. Tisdale

Sponsorship: NSF Graduate Research Fellowship award no. 1745302, U.S Army Research Office award no. W911NF-23-1-0229

Rapidly expanding integration of semiconductors in consumer electronics up through large-scale supercomputers necessitates substantial quantum efficiency improvements to reduce global electricity consumption. 2D semiconductors, like transition metal dichalcogenides (TMDs) and 2D layered perovskites, have emerged in recent years as strong contenders over silicon and other bulk semiconductors due to their strong exciton binding energy and highly tunable properties.

Our lab investigates metal organic chalcogenolates (MOCs) as 2D semiconductors that can improve upon these existing structures—for example, the layer dependence of TMDs and instability of lead halide perovskites. MOCs are novel van der Waals stacked hybrid organic-inorganic semiconductors with extreme 1D quantum confinement, in-plane

anisotropy, and layer independent emission. These properties are promising for applications as light emitting diodes (LEDs), excitonic switches, and a variety of other optoelectronic devices. Silver phenylselenolate, $[\text{AgSePh}]_\infty$, is a MOC of particular interest due to its narrow, naturally blue emission (~467 nm), along with its high environmental stability from covalently bonded organic and inorganic atoms. However, its excited state dynamics are still dominated by nonradiative recombination mechanisms, limiting its potential to revolutionize future semiconductor frameworks. This work details plans to perform physical, chemical, and electrical manipulation of MOCs to identify the influence of extrinsic defects and intrinsic material properties on exciton mobility and recombination in 2D hybrid semiconductors.

Universal Transferred Process for 2D Materials

S. He, Z. Hennighausen, J. Kong

Sponsorship: U. S. Army Research Laboratory and the U. S. Army Research Office under contract/grant number W911NF2320057

Two-dimensional (2D) materials have garnered significant attention due to their exceptional properties, but preparing with controllable thickness and usable surface area is still challenging. Numerous techniques have emerged for synthesizing high-quality and large-area 2D materials. Among these methods, chemical vapor deposition (CVD) has shown promise, offering superior control over film thickness and uniformity, making it a reliable technology for wafer-scale manufacturing. On the other hand, the typical wet transfer method using PMMA presents a potential solution for transferring 2D materials in large-scale. However, it faces limitations when transferring CVD-synthesized 2D materials

from the growth substrate to the target substrate over large areas while maintaining clean surface. To overcome these challenges, we introduce a universal transfer process to keep clean surface using other polymers within a vacuum environment. Comparing wet-transfer and roll-to-roll transfer with vacuum dry transfer. Furthermore, we investigate the different surface situation of 2D materials using different polymers under atmospheric and vacuum environment. Our proposed method opens new possibilities for residue-free 2D materials on a large scale, with potential applications under diverse environments.

Defects Break the Self-Limiting Nature of the Room-Temperature Atomic-Layer Substitution for Growing Janus Monolayer Transition Metal Dichalcogenides

T. Zhang, X. Zheng, Y. R. Peng, K. Zhang, Y. Zhu, T. H. Yang, H. Liu, S. Y. Tang, Y. Guo, Y. L. Chueh, T. Cao, J. Kong
Sponsorship: US Department of Energy (DOE), Office of Science, Basic Energy Sciences under Award DE-SC0020042.

Janus monolayer transition metal dichalcogenides (J-TMDs) are gaining an increasing attention because of various intriguing properties that arise from their unique asymmetrical structure. A low-energy-barrier room-temperature atomic-layer substitution (RT-ALS) approach has recently been developed to obtain J-TMDs. This method reliably converts either MS_2 or MSe_2 (M represents a metal atom) into $MSSe$ -type J-TMDs with controlled out-of-plane dipole orientations. Theoretical calculations based on a perfect monolayer TMD lattice model have illustrated that the RT-ALS reaction is self-limiting, in which only the top-most layer of chalcogen atoms is substituted. However, it remains unexplored how the atomic defects in monolayer TMDs affect the RT-ALS reaction pathway and the resulting J-TMDs' crystal quality.

Herein, we studied the role of defects on the

RT-ALS process using high-quality and defect-rich $MoSe_2$, synthesized by a recently devised defect-engineered growth approach, as starting materials. Very interestingly, we found that an increased defect density in the starting material breaks the self-limiting nature of RT-ALS, leading to the incorporation of S in the bottom atomic layer of the as-synthesized Janus $MoSeS$. Our results indicate a positive correlation between the qualities of starting material and resulting J-TMDs, and suggest a defect-mediated atomic substitution pathway that has not been considered before. Our study contributes to the understanding and optimization of J-TMD preparation strategies to make these materials ready for constructing novel electronics, photonics, and Moiré heterostructures in the future.

Elucidating the Role of MOF Pore Size on OSN Performance of Microporous Polymer-based Mixed-matrix Membranes

W. Wu, T. H. Lee, G. Dovranova, A. Hernandez, Z. P. Smith
Sponsorship: ExxonMobil

Organic solvent-based separations are ubiquitous in the chemical industry, but they often rely on energy-intensive processes. Membrane technology provides an energy-efficient alternative to offset the energy cost. However, developing highly selective membranes for organic solvent nanofiltration (OSN) has been a significant challenge due to the poor stability of polymers under aggressive solvent conditions. Mixed-matrix membranes (MMMs) based on fillers such as metal-organic frameworks (MOFs) with well-defined porous structures have shown promise in overcoming these limitations. While material design efforts have improved OSN performance with MMMs, the fundamental mechanisms behind the effects of filler incorporation on solvent transport are not yet fully understood. In this study, we aim to elucidate the effects of MOF pore size on OSN performance for microporous polymer-based MMMs.

A series of MOF nanoparticles with similar chemistry but systematically increasing pore sizes

(UiO-6x-NH₂ (x=6,7,8)) were chosen for this work. A carboxylic acid functionalized PIM-1 polymer (PIM-COOH) and the MOF nanoparticles were fabricated into thin-film MMMs using a newly developed spin-casting process followed by a crosslinking reaction. Dead-end permeation tests showed lower methanol permeability in all the MMMs compared to their polymer counterparts due to the restricted membrane swelling in the presence of MOF. The molecular weight cutoff (MWCO) of MMMs was probed through the permeation of dyes in methanol, revealing that the highest MWCO values were found for MMM samples with poor interfacial compatibility, indicating that unrestricted polymer swelling and defects need to be carefully controlled to enable MOF-based MMMs for OSN applications. For the MMMs with compatible interfaces, this study provides structure-property guidelines on the role of systematically increased MOF pore apertures and OSN separation performance.

Implementation of Multi-functional Diffractive Optical Elements by Implosion Fabrication

G. Yang, Q. Yang, Y. Salamin, Y. Kunai, T. Nambara, P. T. C. So, E. S. Boyden
Sponsorship: Fujikura

The development and integration of miniaturized holography and diffractive lenses represent an emerging field in optical technology. Nanofabrication technology plays a crucial role in enabling the design of optical systems at the nanoscale, facilitating the creation of structures and devices with unmatched precision and functionality. Despite this, current nanofabrication methods encounter challenges in crafting complex free-form three-dimensional (3D) structures and in constructing multi-layer, multi-level features at the nanoscale. We propose the use of implosion fabrication (ImpFab) to over-come these limitations, allowing the production of nano-optics that surpass the diffraction limits of direct laser writing (DLW) and enable the assembly of nano-precise, highly flexible 3D architectures.

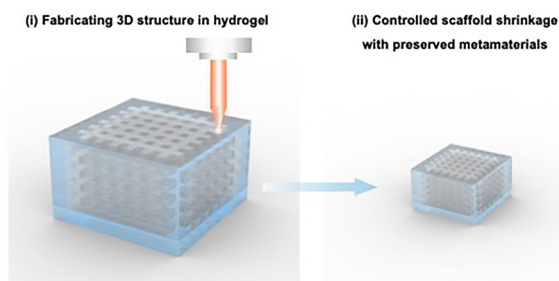
In the ImpFab process (Figure 1), a hydrogel matrix undergoes selective photo-ablation in targeted areas using a two-photon laser, forming non-self-supporting 3D topological features. This matrix is then isotropically shrunk to achieve nano-precise features, essential for manipulating the critical refractive index (RI) differences required for advanced nanophotonics applications.

We initially constructed a Fresnel lens with three layers and four grayscale levels, achieving feature sizes as small as 200 nm laterally and 1 μm axially. The pre-shrinkage structures, visualized in the fluorescent

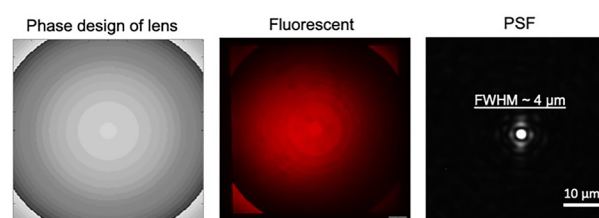
images of Figure 2, closely correspond to the intended morphology and design patterns. Post-shrinkage, the lens retains detailed structural integrity. Performance evaluations through point spread function (PSF) testing confirmed that the focusing capabilities of the lens align with our design expectations.

Building on this, we developed a grayscale holographic device atop the lens layer. Illustrated in Figure 3, this device features a metasurface with a resolution of 100 nm, eight grayscale levels, and a step size of 200 nm, prominently displaying a simulated reconstruction of the MIT logo. Microscopic imaging of these metasurface nanostructures showed precise alignment with our design specifications. Far-field diffraction imaging tests of the holographic device revealed that it successfully diffracts light to reconstruct and project the encoded MIT logo pattern.

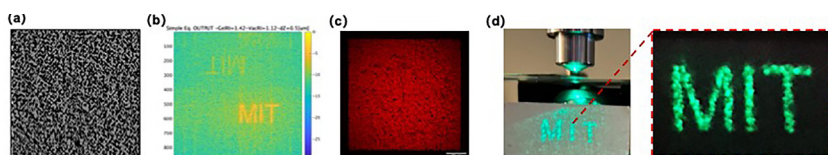
These demonstrations validate that ImpFab technology can achieve nanoscale optical integration. Ongoing advancements in ImpFab are paving the way for the integration of sophisticated, miniaturized optical elements such as holography and diffractive lenses, offering significant improvements in performance, efficiency, and application diversity. This technology effectively addresses the limitations of 3D nano-optics fabrication, heralding a new era in nanophotonics.



▲ Figure 1: Fabrication process of nanoscale topological 3D structure in hydrogel scaffolds.



▲ Figure 2: Diffractive lens design (left), fluorescent image of patterned structure (middle) and performance of PSF (right).



◀ Figure 3: a) Designed mask of holographic metasurface; b) Simulated image of reconstructed MIT logo; c) Fluorescent image of plane of patterned layer; d) Far-field diffraction effect, displayed as MIT logo.

FURTHER READING

- D. Oran, S. G. Rodriques, R. Gao, S. Asano, M. A. Skylar-Scott, F. Chen, P. W. Tillberg, A. H. Marblestone, and E. S. Boyden, "3D Nanofabrication by Volumetric Deposition and Controlled Shrinkage of Patterned Scaffolds," *Science*, vol. 362, pp. 1281-1285, Dec. 2018.

Large Quantum Anomalous Hall Effect in Spin-orbit Proximitized Rhombohedral Graphene

T. Han, Z. Lu, Y. Yao, J. Yang, J. Seo, C. Yoon, K. Watanabe, T. Taniguchi, L. Fu, F. Zhang, L. Ju
Sponsorship: Sloan Fellowship, NSF

In 1988, Haldane proposed a prototype model to realize quantized Hall conductance in the absence of a magnetic field. The model has informed the theoretical and experimental exploration of topological phases of matter for more than three decades. Although the Berry curvatures of the Haldane model have been demonstrated in a cold-atom experiment, the quantum anomalous Hall effect (QAHE), as the most prominent macroscopic signature of the Haldane model, could not be measured there. In solid-state systems, the QAHE has been observed in two categories of materials. The first is magnetic topological insulators such as Cr-/V doped $(\text{Bi,Sb})_2\text{Te}_3$ and intrinsic MnBi_2Te_4 , where the time-reversal-symmetry is broken by the ordering of magnetic elements and the Berry curvatures of the two valleys of opposite surfaces add up to a Chern number of 1. The second is two-dimensional materials with moiré superlattices at non-zero charge densities that correspond to odd filling factors, where the exchange interactions spontaneously break the time-reversal-symmetry and the Chern number arises from a single principal valley. Without the stacking of multiple (effectively decoupled) periods of molecular-beam-epitaxy-grown quantum wells in the vertical direction, the

largest Chern number that has been realized so far is 2 in ferromagnetic systems that were not fully quantized at zero magnetic field. Is it possible to realize the QAHE without magnetic elements or moiré engineering? Can we get a larger Chern number in other QAHE systems? Such possibilities have remained elusive experimentally, although an integer QAHE in rhombohedral graphene was predicted to be possible by theory.

We report the QAHE in a rhombohedral pentalayer graphene/monolayer WS_2 hetero-structure. Distinct from other experimentally confirmed QAHE systems, this system has neither magnetic element nor moiré superlattice effect. The QAH states emerge at charge neutrality and feature Chern numbers $C = \pm 5$ at temperatures up to about 1.5 K. This large QAHE arises from the synergy of the electron correlation in intrinsic flat bands of pentalayer graphene, the gate-tuning effect, and the proximity-induced Ising spin-orbit-coupling. Our experiment demonstrates the potential of crystalline two-dimensional materials for intertwined electron correlation and band topology physics and may enable a route for engineering chiral Majorana edge states.

FURTHER READING

- T. Han, et al, "Large Quantum Anomalous Hall Effect in Spin-orbit Proximitized Rhombohedral Graphene," *Science*, arXiv preprint arXiv:2310.17483 (2023), in press.